

ORIGINAL ARTICLE

Thiophene substituted phenothiazine polymers: Design, synthesis and characterization



Ruhiye Nilay Tezel^{a,b}, İsmet Kaya^{a,*}

^a Çanakkale Onsekiz Mart University, Department of Chemistry, Polymer Synthesis and Analysis Laboratory, 17020 Çanakkale, Turkey

^b Çanakkale Onsekiz Mart University, Lapseki Vocational School, Department of Chemistry and Chemical Processing Technologies, Çanakkale, Turkey

Received 18 November 2017; accepted 19 September 2018

Available online 25 September 2018

KEYWORDS

Phenothiazine;
Oxidative polymerization;
Fluorescence;
Thermal analysis;
SEM

Abstract In this paper, the polymers containing phenothiazine were synthesized via oxidative polymerization reaction by FeCl_3 as oxidant. These polymers contain ether unit, aliphatic chain and aromatic groups as bridges in their structures. The effects of the groups on the optical, thermal, morphological properties of the polymers were investigated. The physical and chemical properties of the monomers and the polymers were identified by FT-IR, NMR, UV-Vis, thermogravimetry (TG), cyclic voltammetry (CV), fluorescence analysis. According to the fluorescence analyses, polymer containing aliphatic ether bridge emitted yellow colour based on the turning of excitation wavelength. The yellow solution of polymer containing aliphatic ether bridge turned into turquoise when excited with the wavelength of 365 nm. Thermal analyses demonstrated that polymer containing phenyl bridge compound had 38% residue amount. Due to fluorescent and thermal properties, these polymers could be used in various applications such as spectrofluorometric ion sensor and polymeric light emitting diodes (PLEDs) with yellow and turquoise emissions.

© 2018 Production and hosting by Elsevier B.V. on behalf of King Saud University. This is an open access article under the CC BY-NC-ND license (<http://creativecommons.org/licenses/by-nc-nd/4.0/>).

1. Introduction

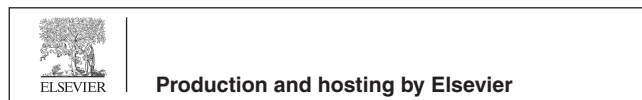
Polymeric materials have played growing significant roles for the requirements of modern society owing to their arrangeable optoelectronic properties, ease of processing, flexibility and

good cost efficiency (Jin et al., 2015). Phenothiazine is a heterocyclic compound which includes a nitrogen atom with lone-pair electrons and electron-giving sulfur atom. This compound exhibits intense luminescence, good hole transport capacity and high photo conductivities (Gao et al., 2016; Hsieh et al., 2015). Generally, phenothiazine derivatives have a low oxidation potential and a high tendency to form stable radical cations (Hsieh et al., 2015). Because of the low oxidation potential and a high tendency to form stable radical cations, appropriate substituted phenothiazine derivatives may find applications in material science investigations. Phenothiazine and its derivatives are used in various areas such as probes, dyes, electrochemistry and pharmaceuticals (Vengaiyan et al.,

* Corresponding author.

E-mail address: ikaya@comu.edu.tr (İ. Kaya).

Peer review under responsibility of King Saud University.



2015). Due to unexcelled optical and electronic properties, polymers containing phenothiazine unit were potential candidate materials for PLEDs (Quiao et al., 2010). Phenothiazine unit containing polymers are also used for applications in the field of OLED, as NIR emitting materials and BHJ solar cells as donor materials (Maglione et al., 2017).

Polymers have been synthesized via several methods such as oxidative polymerization in the presence of FeCl_3 , transition-metal-catalyzed reactions (Yamamoto and Suzuki coupling reactions), elimination of HBr and electropolymerization (Kaya et al., 2013). Compared with these polymerization methods, oxidative polymerization using ferric (III) chloride (FeCl_3) is easy and cheap with moderate reaction conditions (at room temperature) (Kocaeren, 2016). Ferric chloride is a well-established reagent for oxidative couplings leading to new C—C bonds (Sarhan et al., 2009).

In this study, aliphatic and aromatic bridging monomers containing phenothiazine unit were synthesized and converted into corresponding polymers via oxidative polymerization with FeCl_3 . These polymers include the ether bridge, aliphatic chain and aromatic groups as bridges in their structures. For this purpose, firstly 3,7-dibromo-10-H-phenothiazine was synthesized using NBS. Then, 3,7-dithien-2-yl-10-H-phenothiazine was synthesized via Suzuki coupling reaction with palladium catalyst. The third step was the synthesis of the product by reaction with dihalogene compounds of 3,7-dithien-2-yl-10-H-phenothiazine. Finally, polymers were synthesized by the oxidative polymerization reaction with ferric (III) chloride (FeCl_3). Monomers and polymers were characterized by FT-IR, NMR, UV-Vis, CV, SEC, SEM, fluorescence and thermal analyses. Difference on photophysical, electrochemical, morphological and thermal properties of the synthesized polymers related to different aliphatic and aromatic groups in the structure were investigated.

2. Experimental

2.1. Materials

Phenothiazine, 2-ethoxyethanol, 1,4-diiodobenzene, 1,4-bis (bromomethyl)benzene, sodium hydride, tetrakis(triphenylphosphine)palladium (0), Iron (III) chloride were purchased from Sigma Aldrich, whereas N-bromosuccinimide (NBS), 1,2-bis (2-chloroethoxy)ethane and 1,5-dibromopentane were bought from Alfa Aesar. 2-thienylboronic acid was provided by Across. All solvents described herein were purchased from Merck Chemical Co. (Germany) and used without any purification.

2.2. Characterization techniques

FT-IR spectra of the synthesized monomers and polymers were recorded on a Perkin Elmer Spectrum One over the range of $4000\text{--}500\text{ cm}^{-1}$. ^1H NMR and ^{13}C NMR spectra were recorded on a JEOL ECX-400 II spectrometer at room temperature in $\text{DMSO-}d_6$ as a solvent. Ultraviolet-visible (UV-Vis) spectra were measured by Analytikjena Specord 210 Plus to study the electronic transition of all compounds with conjugated π systems. Emission and excitation spectra of the synthesized monomers and polymers were determined by Shimadzu RF-5301PC Spectrofluorophotometer. Thermogravimetry

analyses (TGA) were performed in nitrogen atmosphere (200 mL min^{-1}) at a heating rate of $10\text{ }^\circ\text{C min}^{-1}$ from $20\text{ }^\circ\text{C}$ to $1000\text{ }^\circ\text{C}$ with a Perkin Elmer Diamond Thermal Analysis System. Electrochemical studies of the synthesized compounds were performed using CHI 660C Electrochemical Analyzer (CH Instruments, Texas, USA). A three electrode system was used for cyclic voltammetry (CV) measurements, which glassy carbon electrode (GCE), Pt wire and Ag/AgCl as working, counter and reference electrode, were used. The HOMO-LUMO energy levels and electrochemical band gaps (E'_g) of monomers and polymers were calculated from oxidation and reduction onset values. Molecular weights were determined by Viscotek GPC max Auto sampler system. Surface morphology of the polymers were determined by using a JEOL JSM-7100F field emission scanning electron microscope.

2.3. Synthesis of the starting materials

3,7-dibromo-10H-phenothiazine (DBP) (Hsieh et al., 2015) and 3,7-Dithienyl-10H-phenothiazine (DTP) were synthesized according to literature (Hemgesberg et al., 2013). The structures of the synthesized compounds were confirmed by FT-IR, ^1H NMR and ^{13}C NMR spectra.

For DBP FT-IR (cm^{-1}): $3337\text{ } \nu$ (N—H), $1592\text{--}1441\text{ } \nu$ (C=C), $1311\text{ } \nu$ (C—N), $737\text{ } \nu$ (C—S) $649\text{ } \nu$ (C—Br). ^1H NMR ($\text{DMSO-}d_6$, δ , ppm): 8.85 (s, 1H, N—H), 6.59 (d, 2H), 7.11 (s, 1H), 7.14 (dd, 2H). ^{13}C NMR ($\text{DMSO-}d_6$, δ , ppm): 141.43, 130.12, 128.62, 118.72, 116.55, 113.19.

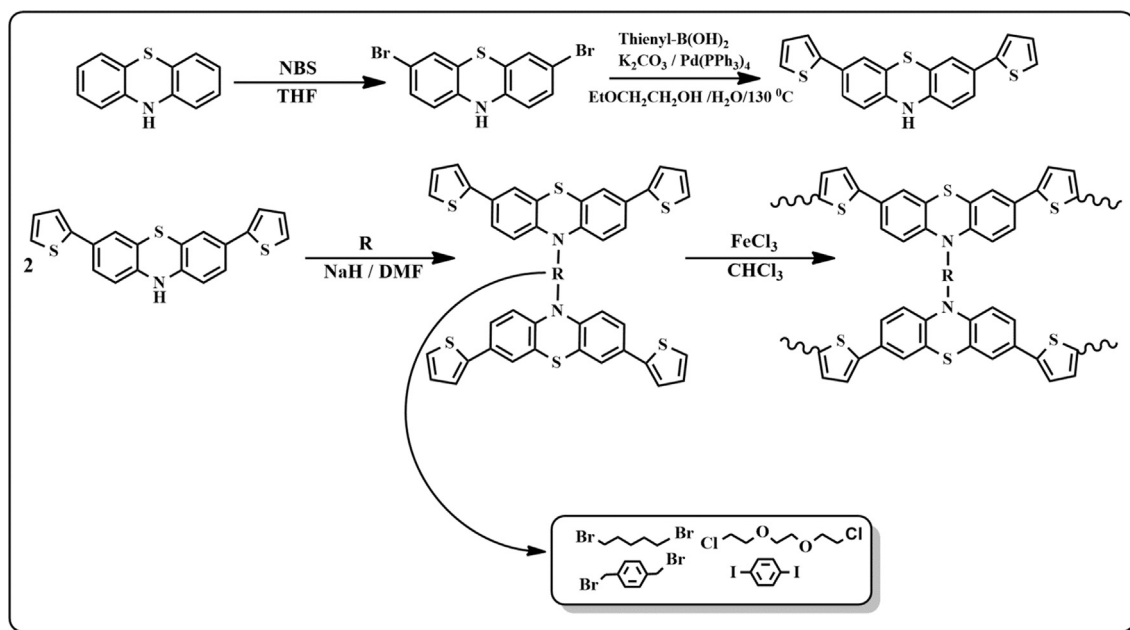
For DTP FT-IR (cm^{-1}): $3364\text{ } \nu$ (N—H), $1590\text{--}1465\text{ } \nu$ (C=C), $1298\text{ } \nu$ (C—N), $798\text{ } \nu$ (C—S). ^1H NMR ($\text{DMSO-}d_6$, δ , ppm): 8.96 (s, 1H, N—H), 7.49 (d, 2H), 7.42 (d, 2H), 7.33 (s, 2H), 7.13 (t, 2H), 6.75 (d, 2H). ^{13}C NMR ($\text{DMSO-}d_6$, δ , ppm): 143.12, 141.10, 128.86, 128.30, 125.50, 124.88, 123.36, 122.89, 117.17, 115.25.

2.4. Synthesis of the aliphatic and aromatic bridging phenothiazine monomers

3,7-dithienyl-10H-phenothiazine (0.36 g, 1 mmol) and sodium hydride (60% dispersion in mineral oil) (0.24 g, 6 mmol) were dissolved in 10 mL of DMF under the argon atmosphere at room temperature. After 30 min, dihalogene compound (0.5 mmol) in 5 mL DMF was added into the reaction mixture, which was stirred for 16 h at $90\text{ }^\circ\text{C}$. Then, reaction mixture was cooled to room temperature. This solution was poured into 100 mL of water and product was filtered, dried and recrystallized from CHCl_3 /hexane (1:1). The product was dried in a vacuum oven at $70\text{ }^\circ\text{C}$ (Jo et al., 2015). This step was repeated separately for each compound. The yields of BDTPP, BDTPPEE, BDTPPB and BDTPMB were found to be 60, 65, 53 and 45%, respectively. Melting points values of BDTPP, BDTPPEE, BDTPPB and BDTPMB were found to be between 181 and $183\text{ }^\circ\text{C}$, $170\text{--}171\text{ }^\circ\text{C}$, $216\text{--}217\text{ }^\circ\text{C}$ and $222\text{--}224\text{ }^\circ\text{C}$, respectively.

2.5. General procedure for the polymerization reaction

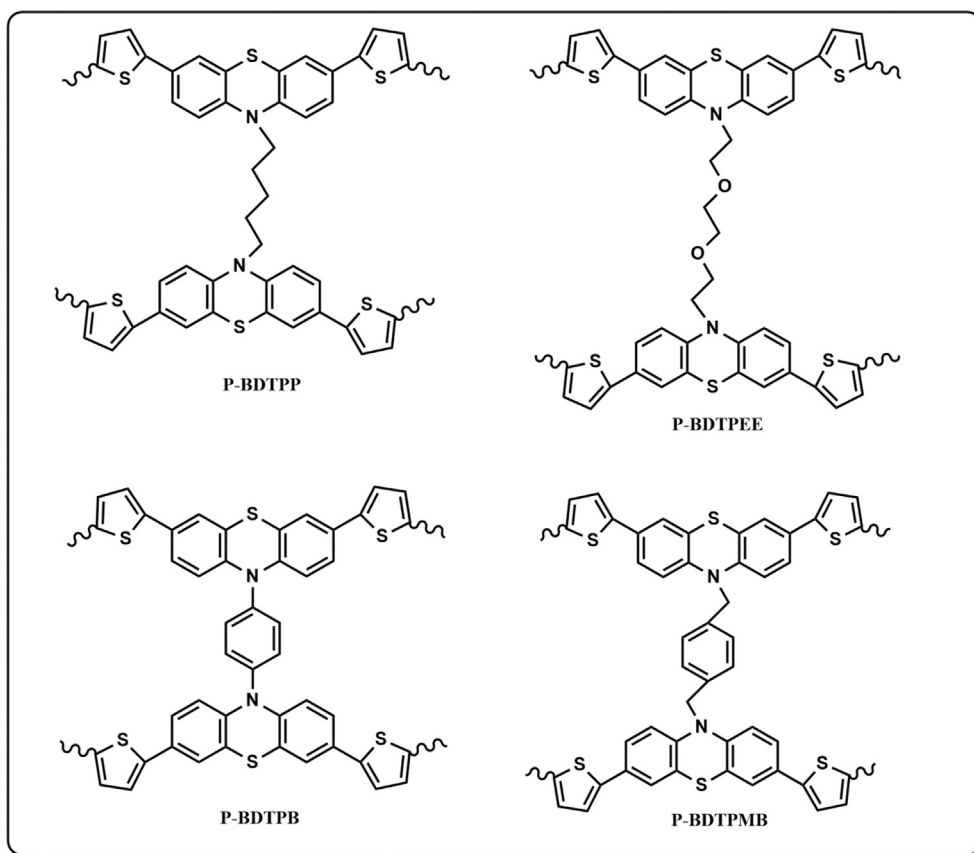
To a suspension of FeCl_3 (0.810 g, 5 mmol) in chloroform (10 mL), 0.5 mmol phenothiazine monomer was added under argon atmosphere. The reaction mixture was stirred for 72 h at room temperature. This solution was then diluted with



Scheme 1 Synthetic pathway of the compounds.

chloroform and washed with water. The organic phase was separated and stirred with ammonia (aq. 20%, 2×100 mL) for 30 min. Then, 0.2 M ethylene-diamino-tetra-acetic acid (EDTA) solution (100 mL) and water (100 mL) were added into the solution. The solution was poured into methanol and

the product was collected by centrifugation (Aydm et al., 2013). The yields of P-BDTPP, P-BDTPEE, P-BDTPB and P-BDTPMB were found to be 48, 50, 45 and 43%, respectively. The general synthetic methods of compounds and structures of the polymers are shown in Schemes 1 and 2, respectively.



Scheme 2 The structures of synthesized polymers.

Table 1 FT-IR spectral data of other monomers and polymers.

Compounds	Ar···CH	Al···CH	—C=C—	C—S	C—N	HC=N—	C—C coupling
BDTPP	3055	2855–2930	1470–1592	795	—	1620	—
P-BDTPP	3060	2859–2927	1472–1595	796	—	1623	1090
BDTPB	3060	—	1496–1580	804	—	1621	—
P-BDTPB	3068	—	1498–1584	807	—	1624	1075

3. Results and discussion

3.1. Structural characterization of the synthesized compounds

The FT-IR spectral data of the synthesized compounds are given in Table 1. According to Table 1, the characteristic peaks like aromatic and aliphatic C—H stretching, C—C coupling peaks are observed as expected. The FT-IR spectra of the starting compounds DBP and DTP are given in Fig. 1. FT-IR spectrum of DBP, which possesses an N—H stretching peak and C—Br stretching peak at 3337 and 649 cm^{-1} respectively, as shown in Fig. 1. DTP possesses N—H stretching peak and C—S stretching peak at 3364 and 798 cm^{-1} respectively. This result showed that bromine was not bound at N position. Fig. 2 shows FT-IR spectra of the 1,2-bis(2-chloroethoxy) ethane (BDTPEE) and 1,4-bis(bromomethyl)benzene (BDTPMB) bridged monomers and polymers. As shown in Fig. 2, while —NH peak disappears, aliphatic and aromatic C—H stretching peaks appear in the structure of monomer and polymer. After the polymerization of each monomer, C—C coupling peaks were observed at around 1070 cm^{-1} . In addition, imine (HC=N) peaks were observed at around 1620 cm^{-1} due to conjugation in phenothiazine ring. The broad bands of the polymers are related to the polyconjugation in the polymer structures. As seen Table 1, other compounds have similar results as expected. While aromatic and aliphatic C—H peaks were observed at around 3055 cm^{-1} and 2934 cm^{-1} respectively, the peaks at 1441–1592 cm^{-1} were attributed to C=C stretching frequency of benzene ring for all the compounds.

The solubility behavior of the synthesized compounds is investigated in different solvents and the results are presented

in Table 2. Generally, all compounds were soluble in polar organic solvents such as DMF, DMSO and DMA.

^1H NMR and ^{13}C NMR spectra of BDTPEE and P-BDTPEE data are given in Figs. 3 and 4, respectively. As seen in the ^1H NMR spectra of BDTPEE, the proton values of aromatic units were observed at 7.16–7.59 ppm. In addition, the aliphatic peaks were observed at 1.35–3.85 ppm. After the polymerization, the signal of the H_g proton at 7.59 ppm as doublet in the BDTPEE compound disappeared, and the signal of H_f proton at 7.16 ppm as triplet in BDTPEE compound was observed at 7.30 ppm as doublet in the polymer compound. The ^{13}C NMR spectrum of BDTPEE indicated that carbon atoms of the aliphatic chain were observed at 58.80–69.90 ppm while the aromatic carbon atoms were observed at 118–146 ppm. The ^{13}C NMR spectrum of P-BDTPEE showed the resonance signals of aromatic carbon atoms at 120–148 ppm whereas carbon atoms of aliphatic chain were observed at 60–69 ppm. Additionally, in the ^{13}C NMR spectrum of the P-BDTPEE a significant decline in the intensity of C_{10} was observed compared to monomer. These results indicate that polymerization takes place predominantly at C_{10} of thiophene units. The NMR analyses data of the synthesized compounds are listed in Table 3.

3.2. Optical and electrochemical properties

Fig. 5 shows the UV–Vis spectra that are measured for the monomers and polymers in DMSO. Band gaps of the monomers and the polymers were estimated from low energy band edges from UV–Vis absorption spectra using the following equation in the literature (Colladet et al., 2004) and were given in Table 2.

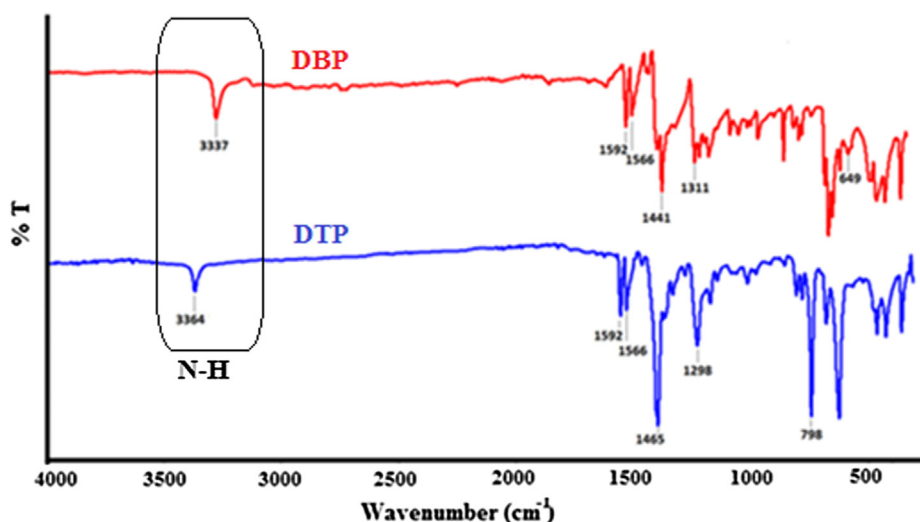


Fig. 1 FT-IR spectra of DBP and DTP.

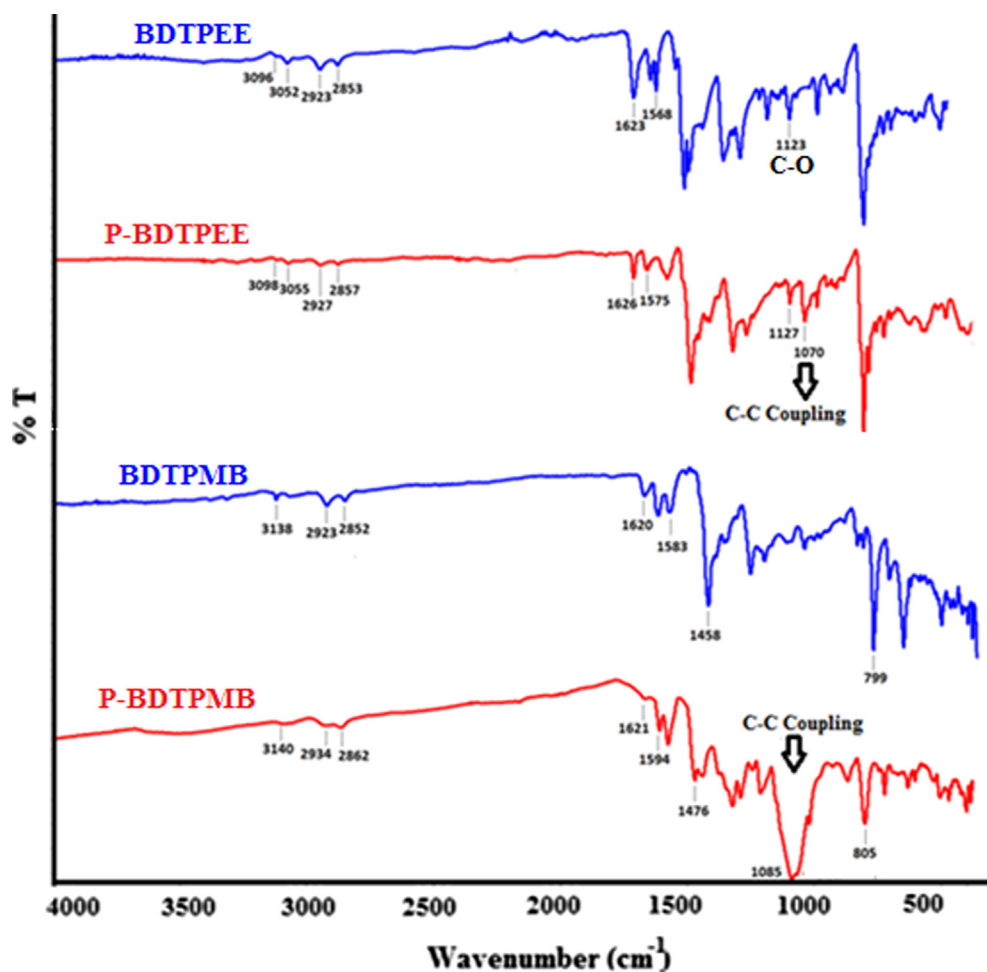


Fig. 2 FT-IR spectra BDTPEE and BDTPMB monomers and their polymers.

$$E_g = 1242/\lambda_{\text{onset}} \quad (1)$$

According to UV-Vis spectra, a red shift occurs at the absorption edge of polymers compared to monomers due to polyconjugation (Kaya et al., 2013). Moreover, the calculated optical band gaps of polymer had lower than those of monomers. It suggested that the increase of phenothiazine-thiophene units resulted in the decrease of E_g due to extending of the conjugated length of polymers (Qui et al., 2007).

According to the obtained spectra, the band above 280 nm is mainly owing to an $n \rightarrow \pi^*$ transition because of the presence of lone electron pairs of sulfur atom in the phenothiazine ring (Manju et al., 2012). The peak at 308–410 nm is formed because of a delocalized $\pi \rightarrow \pi^*$ transition along the polymer chain, and the peak at 460–545 nm is induced from a localized transition at the state of charge transfer between phenothiazine and thiophene rings (Yun et al., 2013).

Table 2 Solubility properties of synthesized compounds.

Compound	Acetonitrile	Acetone	n-Hexane	EtOAc	DMF	DMSO	THF	DMA
BDTPP	⊥	+	–	+	+	+	+	+
P-BDTPP	–	–	–	⊥	+	+	+	+
BDTPEE	⊥	+	–	+	+	+	+	+
P-BDTPEE	–	⊥	–	⊥	+	+	+	+
BDTPB	–	+	–	+	+	+	⊥	+
P-BDTPB	–	–	–	⊥	+	+	–	+
BDTPMB	–	+	–	+	+	+	⊥	+
P-BDTPMB	–	–	–	⊥	+	+	–	+

–: insoluble, ⊥: moderate solubility, +: solubility.

Cyclic voltammetry (CV) was carried out to investigate electrochemical properties of the synthesized monomers and polymers. As seen in Fig. 6, all compounds have two oxidation peaks except BDTPP monomer and its corresponding polymer. BDTPP monomer and its corresponding polymer have pentane chain as bridge. This means that, after the oxidation of the phenothiazine core the electron density of BDTPP compound is not sufficiently high to allow thiophene oxidation. When Fig. 6 is examined, the oxidation potential of the polymer compounds lower values compared to that of the monomer compounds. Since thiophene is a relatively electron-rich, the thienyl units should thus induce a much higher electron density within the phenothiazine, making it much more suscep-

tible towards oxidation (Hemgesberg et al., 2013). From the onset, oxidation and reduction peak potentials HOMO-LUMO energy levels and electrochemical band gaps (E'_g) were calculated as shown in Table 4. To calculate these parameters, the following equations were used (Cervini et al., 1997):

$$E_{\text{HOMO}} = -(4.39 + E_{\text{ox}}) \quad (2)$$

$$E_{\text{LUMO}} = -(4.39 + E_{\text{red}}) \quad (3)$$

$$E'_g = E_{\text{LUMO}} - E_{\text{HOMO}} \quad (4)$$

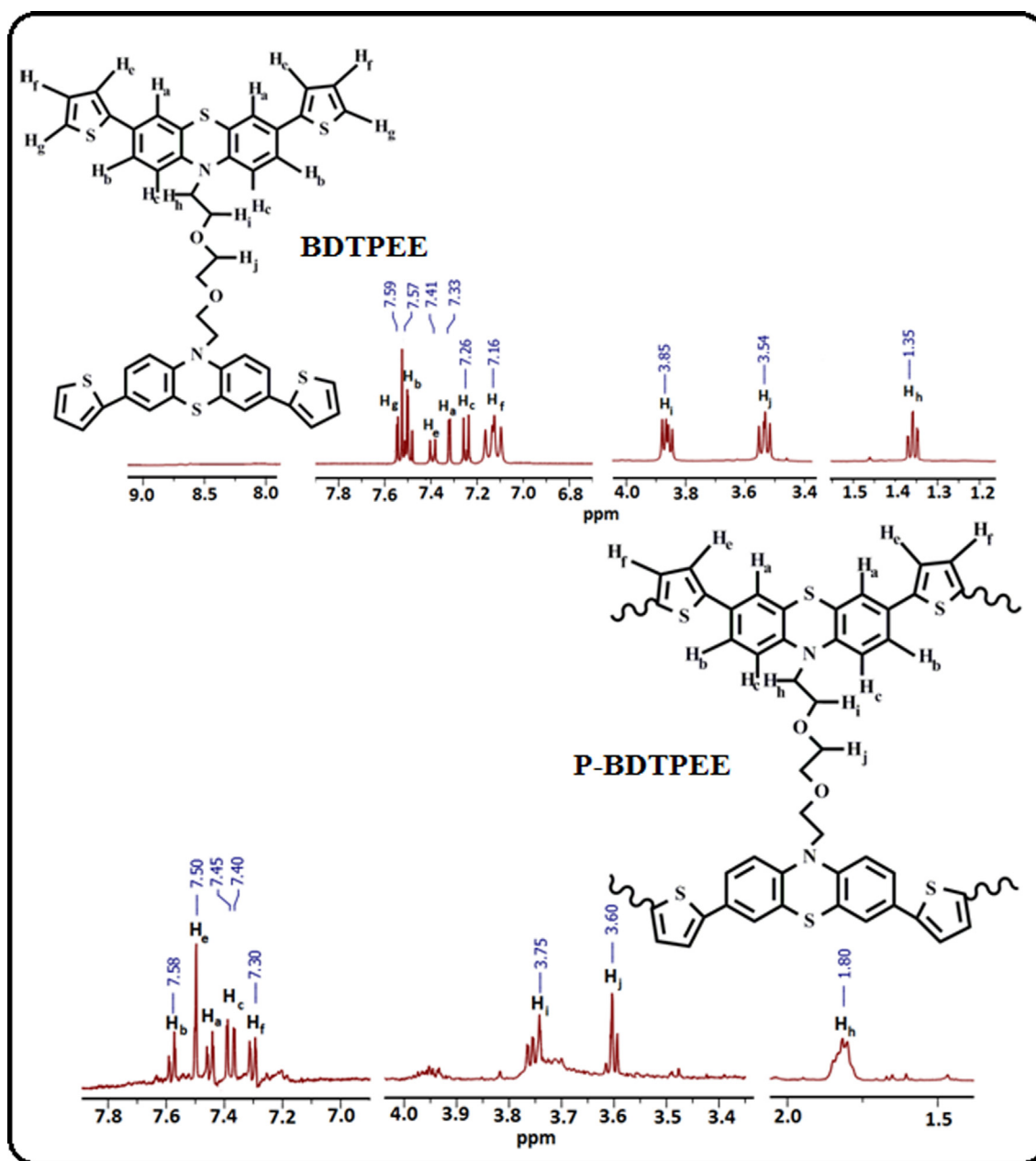


Fig. 3 ^1H NMR spectra of BDTPEE and P-BDTPEE.

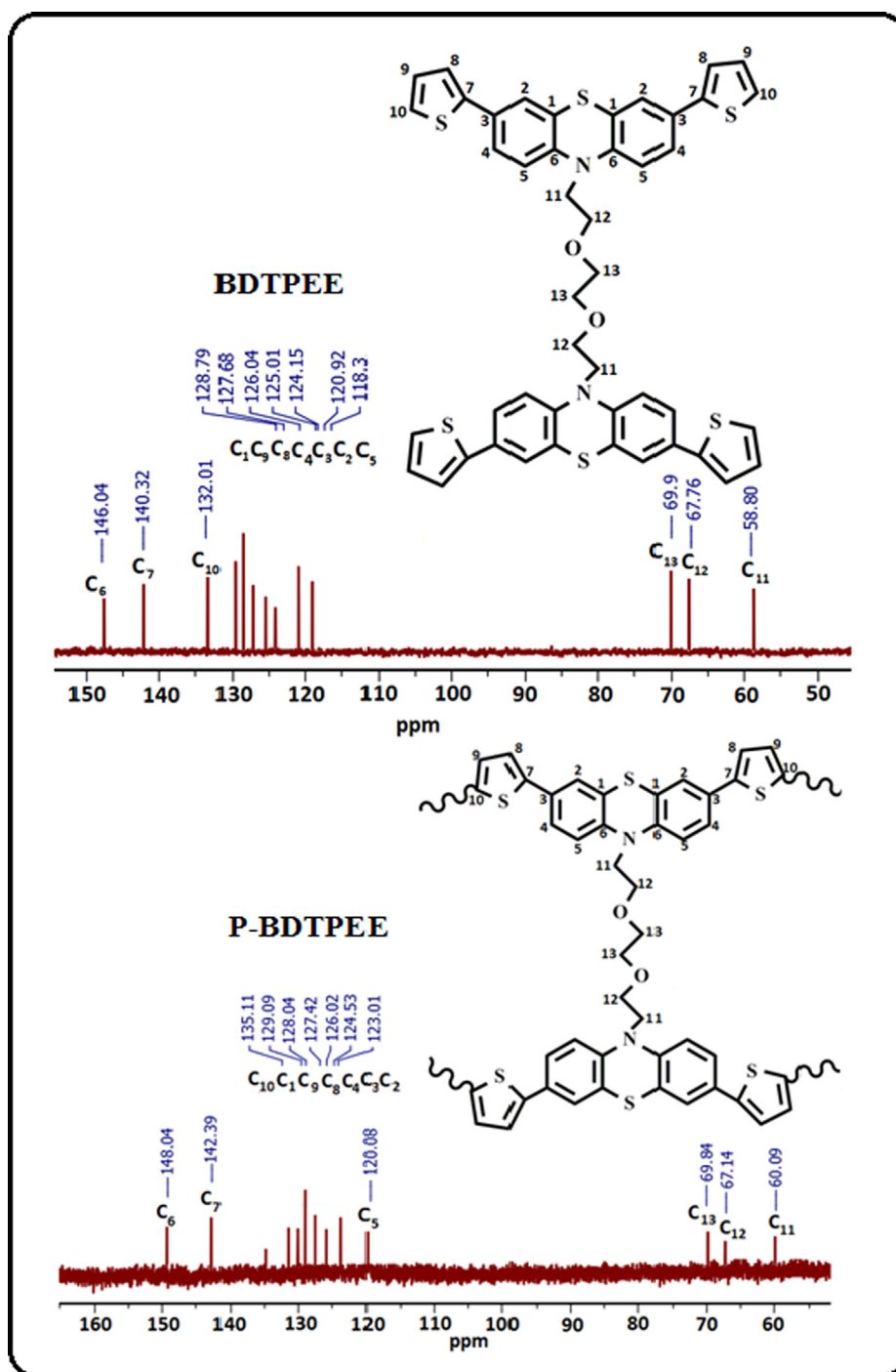


Fig. 4 ^{13}C NMR spectra of BDTPEE and P-BDTPEE.

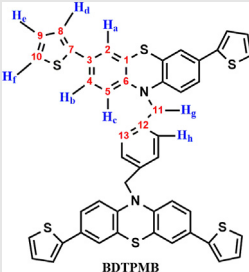
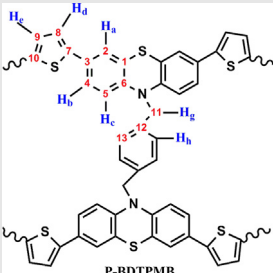
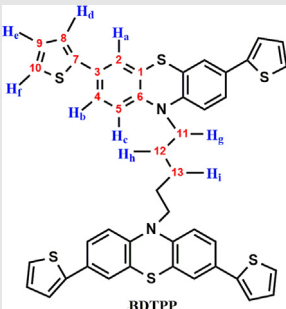
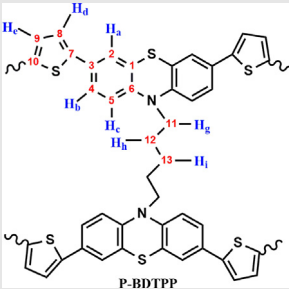
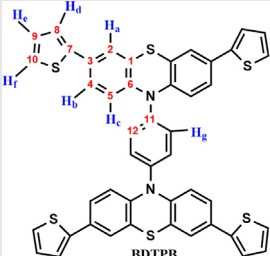
According to Table 4, the electrochemical band gaps (E'_g) of polymers changes are as follows: P-BDTPB < P-BDTPMB < P-BDTPEE < P-BDTPP. P-BDTPP has a bit higher electrochemical and optical band gaps than other polymers. This can be probably because of straight aliphatic structure of P-BDTPP. The observed optical band gaps of polymers are smaller than thiophene substituted phenothiazine polymers in literature the earlier reported (Lin et al., 2015). By using

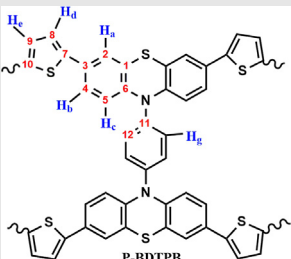
solar cells fabricated from these low bandgap polymers, it is possible to capture more of the solar radiation. (Cai et al., 2010).

3.3. Fluorescence measurement

Fluorescence properties of the synthesized compounds were determined using DMSO solutions. Fig. 7 shows fluorescence

Table 3 NMR spectra data of the synthesized compounds.

Compounds	NMR spectra data (DMSO d_6 , δ , ppm)
 <p>BDTPMB</p>	<p>$^1\text{H NMR}$: 7.60 (d, $-\text{H}_f$), 7.57 (d, $-\text{H}_b$), 7.44 (s, $-\text{H}_a$), 7.40 (d, $-\text{H}_d$), 7.30 (s, $-\text{H}_h$), 7.25 (d, $-\text{H}_c$), 7.20 (t, $-\text{H}_e$), 3.71 (s, $-\text{H}_g$).</p> <p>$^{13}\text{C NMR}$: 145.63 (C₆), 140.82 (C₇), 136.16 (C₁), 132.70 (C₁₀), 130.28 (C₁₃), 128.89 (C₁₂), 127.07 (C₇), 126.78 (C₉), 126.55 (C₂), 124.06 (C₃), 121.37 (C₄), 120.77 (C₅).</p>
 <p>P-BDTPMB</p>	<p>$^1\text{H NMR}$: 7.55 (d, $-\text{H}_b$), 7.47 (s, $-\text{H}_a$), 7.44 (d, $-\text{H}_c$), 7.39 (s, $-\text{H}_i$), 7.32 (d, $-\text{H}_e$), 7.27 (d, $-\text{H}_f$), 3.74 (s, $-\text{H}_h$).</p> <p>$^{13}\text{C NMR}$: 147.42 (C₆), 141.41 (C₇), 138.27 (C₁), 133.76 (C₁₀), 131.87 (C₁₃), 131.19 (C₁₂), 128.93 (C₇), 127.60 (C₉), 127.38 (C₂), 125.11 (C₃), 123.31 (C₄), 121.44 (C₅), 54.37 (C₁₁).</p>
 <p>BDTPP</p>	<p>$^1\text{H NMR}$: 7.62 (d, $-\text{H}_f$), 7.54 (d, $-\text{H}_d$), 7.51 (t, $-\text{H}_e$), 7.37 (d, $-\text{H}_c$), 7.23 (d, $-\text{H}_b$), 7.10 (s, $-\text{H}_a$), 4.32 (t, $-\text{H}_g$), 1.75 (m, $-\text{H}_h$), 1.24 (m, $-\text{H}_i$).</p> <p>$^{13}\text{C NMR}$: 145.95 (C₆), 143.36 (C₇), 132.19 (C₁₀), 130.35 (C₂), 129.59 (C₉), 128.71 (C₈), 125.48 (C₄), 124.78 (C₃), 120.32 (C₅), 117.21 (C₁), 53.55 (C₁₁), 30.73 (C₁₂), 26.69 (C₁₃).</p>
Compounds	NMR spectra data (DMSO d_6 , ppm)
 <p>P-BDTPP</p>	<p>$^1\text{H NMR}$: 7.56 (d, $-\text{H}_d$), 7.52 (d, $-\text{H}_c$), 7.40 (d, $-\text{H}_e$), 7.24 (d, $-\text{H}_b$), 7.12 (s, $-\text{H}_a$), 4.34 (t, $-\text{H}_g$), 1.79 (m, $-\text{H}_h$), 1.28 (m, $-\text{H}_i$).</p> <p>$^{13}\text{C NMR}$: 148.77 (C₆), 145.47 (C₇), 134.15 (C₁₀), 131.73 (C₂), 130.53 (C₉), 129.72 (C₈), 126.58 (C₄), 125.78 (C₃), 122.79 (C₅), 117.51 (C₁), 53.70 (C₁₁), 33.39 (C₁₂), 27.61 (C₁₃).</p>
 <p>BDTPB</p>	<p>$^1\text{H NMR}$: 7.62 (d, $-\text{H}_f$), 7.54 (d, $-\text{H}_d$), 7.41 (t, $-\text{H}_e$), 7.13 (s, $-\text{H}_a$), 7.26 (d, $-\text{H}_c$), 7.23 (d, $-\text{H}_b$), 7.16 (s, $-\text{H}_g$).</p> <p>$^{13}\text{C NMR}$: 144.26 (C₆), 140.91 (C₇), 140.42 (C₁₁), 136.28 (C₁₂), 132.64 (C₁₀), 129.10 (C₉), 128.80 (C₈), 126.73 (C₁), 130.04 (C₂), 125.55 (C₃), 123.68 (C₄), 121.12 (C₅).</p>

Compounds	NMR spectra data (DMSO d_6 , δ , ppm)
	$^1\text{H NMR}$: 7.65 (d, $-\text{H}_d$), 7.56 (d, $-\text{H}_e$), 7.18 (s, $-\text{H}_a$), 7.28 (d, $-\text{H}_c$), 7.26 (d, $-\text{H}_b$), 7.18 (s, $-\text{H}_g$). $^{13}\text{C NMR}$: 145.64 (C_6), 142.48 (C_7), 141.86 (C_{11}), 138.65 (C_{12}), 133.57 (C_{10}), 132.74 (C_9), 129.42 (C_8), 128.52 (C_1), 127.28 (C_2), 126.33 (C_3), 125.47 (C_4), 123.27 (C_5).

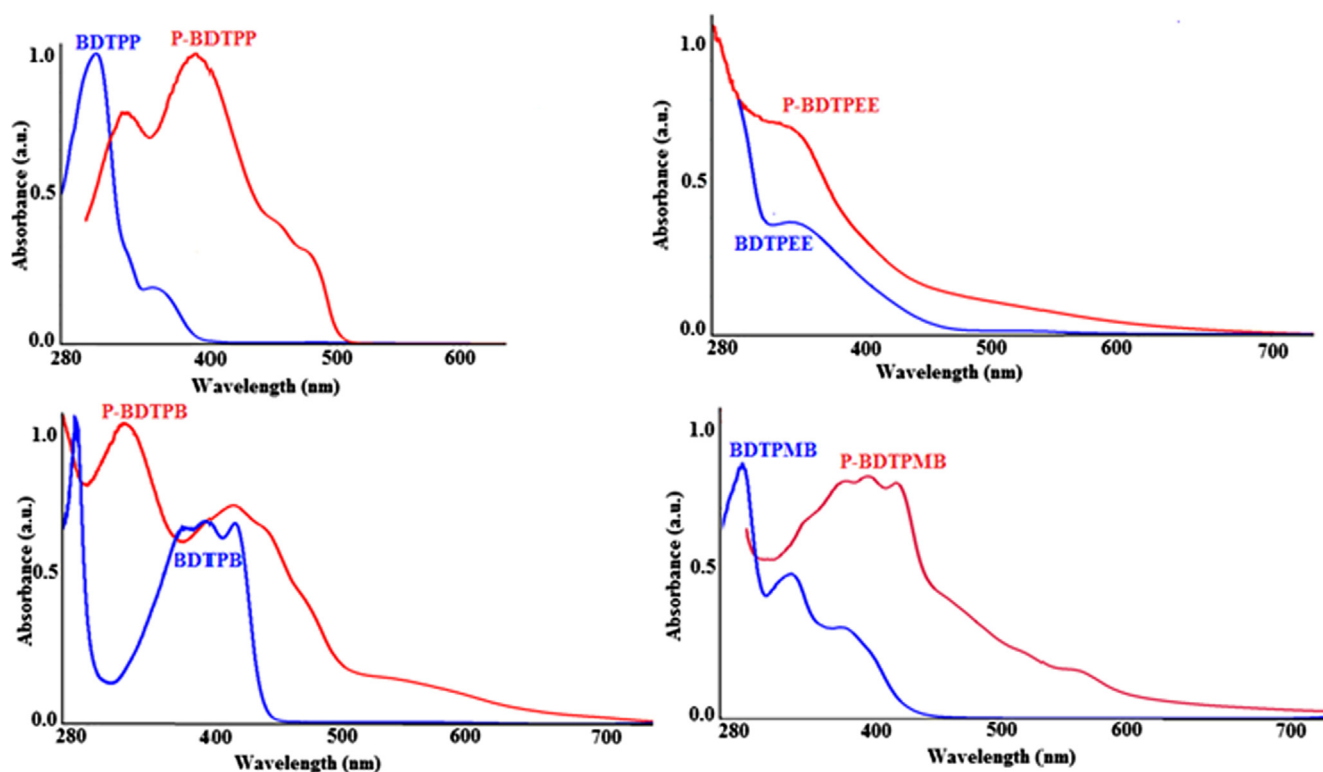


Fig. 5 Absorption spectra of the monomers and polymers.

spectra of synthesized monomers and polymers. The fluorescence intensity was enhanced more significantly from P-BDTPB to P-BDTPMB and less from P-BDTPP to P-BDTPEE, probably because of conjugation. The fluorescence emission bands of the polymers were red-shifted compared to the monomers as shown in Fig. 7. Especially, P-BDTPEE emits light in a wide range from 380 to 505 nm. The shift in emission wavelength from 440 nm to 505 nm in the polymer of BDTPEE compared to the monomer shows that conjugation is higher in the polymer. Additionally, unpaired electron pairs on the oxygen atoms in the ethoxy groups used as bridge in BDTPEE have the ability to increase fluorescence intensity. The obvious reason for the observed red shift is characteristic of donor-acceptor structure, which may effect on their maximal absorption wavelength (Oleksy et al., 2011). Therefore,

the fluorescence intensity of the monomer and polymer of BDTPEE is higher than this of BDTPP. Solution in DMSO of P-BDTPEE has yellow color under sunlight. The yellow solution of P-BDTPEE turned into turquoise when excited with the wavelength of 365 nm (Fig. 8).

3.4. Thermal properties of polymers

TG-DTG-DTA curves of aliphatic and aromatic bridged polymers are shown in Fig. 9. Thermal decomposition data of monomers and polymers are listed in Table 5. As seen in Fig. 9, while BDTPP, BDTPEE, BDTPMB and BDTPB demonstrated two degradation steps, P-BDTPP, P-BDTPEE, P-BDTPMB and P-BDTPB were demonstrated three degradation steps at the same thermal conditions. The initial

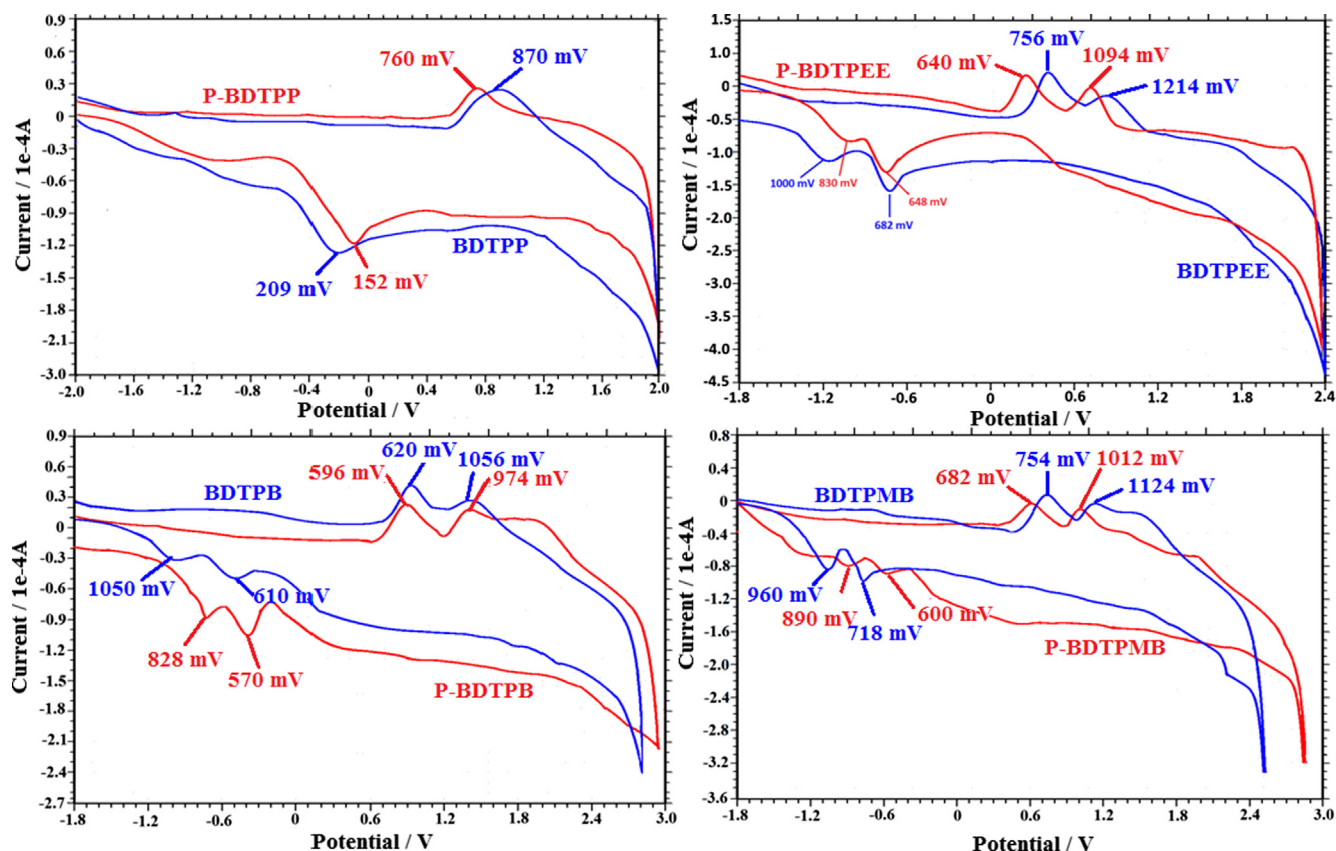


Fig. 6 Cyclic voltammograms of the synthesized compounds.

Table 4 Electronic structure parameters of the synthesized compounds.

Compounds	^a E _{HOMO}	^b E _{LUMO}	^c E _g	^d E _g
BDTPP	-5.26	-2.30	2.96	3.35
P-BDTPP	-5.15	-2.87	2.28	2.42
BDTPEE	-5.60	-3.39	2.21	2.25
P-BDTPEE	-5.48	-3.56	1.92	2.05
BDTPB	-5.44	-3.34	2.10	2.38
P-BDTPB	-5.36	-3.56	1.80	1.92
BDTPMB	-5.51	-3.43	2.08	2.13
P-BDTPMB	-5.40	-3.50	1.90	1.98

^a Highest occupied molecular orbital.

^b Lowest unoccupied molecular orbital.

^c Electrochemical band gap.

^d Optical band gap.

degradation temperatures (T_{on}) of P-BDTPP, P-BDTPEE, P-BDTPMB and P-BDTPB were calculated as 282, 206, 196 and 189 °C, respectively. According to TGA results, the initial degradation temperatures (T_{on}) of BDTPEE and P-BDTPP are higher than those of the other compounds. The % char amounts of P-BDTPP, P-BDTPEE, P-BDTPMB and P-BDTPB were found to be 1.96, 3.75, 32.64 and 61.25, respec-

tively, in the nitrogen atmosphere at 1000 °C. When %char amounts of the polymers are compared, the aromatic bridged polymers had higher %char amounts than those of the aliphatic bridged polymers at 1000 °C. Additionally, %char of P-BDTPMB was higher than the other polymers. This shows that the polymer is thermally stable. The 50% weight loss temperatures of BDTPP, P-BDTPP, BDTPEE, P-BDTPEE, BDTPMB, P-BDTPMB and BDTPB were found to be 219, 422, 322, 848, 555, 428 and 522 °C, respectively. BDTPEE had a weak C—O etheric bond that could be easily broken at moderate temperatures. Also, thermal degradation process of BDTPEE was ended at 550 °C. The lowest % char amount was related to P-BDTPEE among the other polymers. The organic solvent losses of P-BDTPP, P-BDTPEE, P-BDTPB and P-BDTPMB were determined as 4.30, 2.80, 2.00 and 2.35%, respectively, until 150 °C. The glass transition temperatures (T_g) and ΔC_p of P-BDTPEE, P-BDTPP, P-BDTPMB and P-BDTPB were found to be 130, 135, 165 and 182 °C and 0.11, 0.268, 0.014 and 0.33 J g⁻¹ K⁻¹, respectively. According to DSC results of polymers, the glass transition temperatures (T_g) of the aromatic bridged polymers have higher than those of the aliphatic bridged polymers. The glass transition temperature is high due to the stiffness of the polymer chain containing the aromatic structures in the polymer main chain.

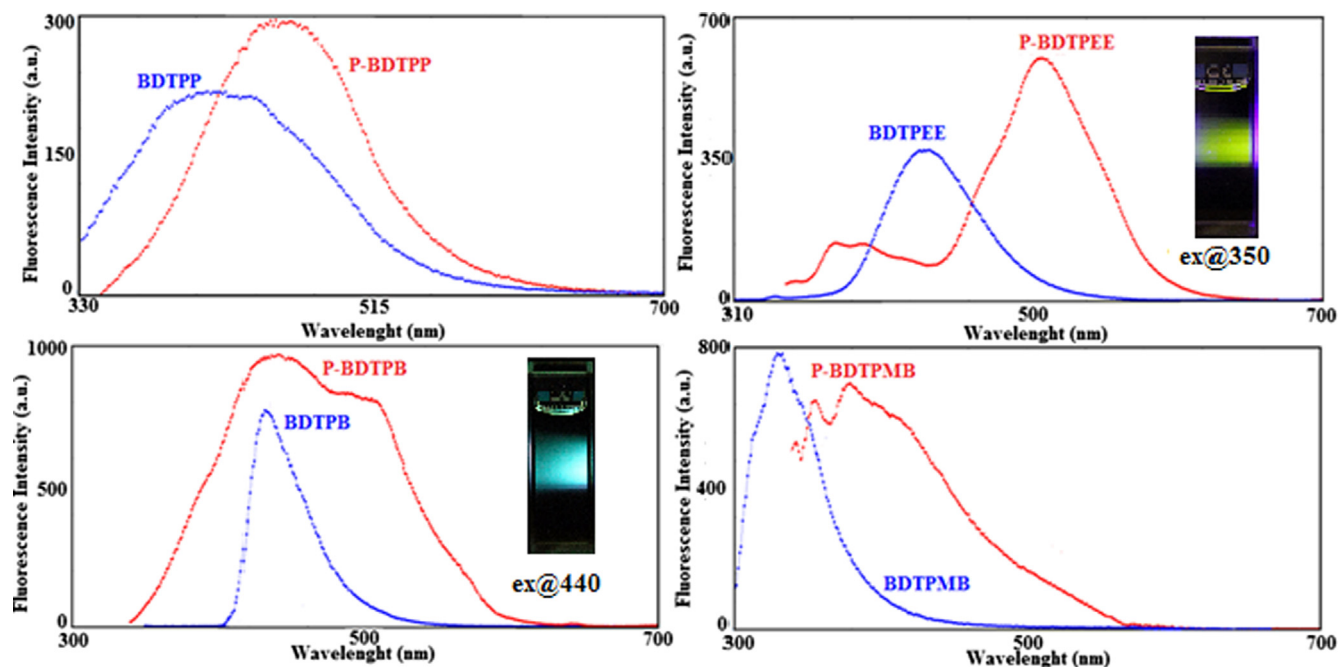


Fig. 7 Fluorescence spectra of the synthesized monomers and polymers in DMF.

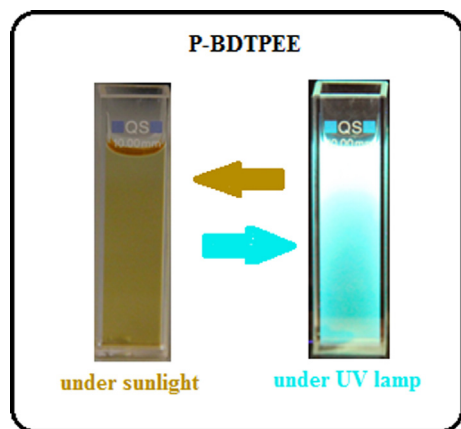


Fig. 8 The colours of P-BDTPEE under sunlight and UV light.

3.5. GPC analysis

The calculated number-average molecular weight (M_n), weight average molecular weight (M_w) and polydispersity index (PDI) values of the polymers were measured by using refractive index detector (RID) in DMF solutions. According to GPC results, the M_w values of P-BDTPP, P-BDTPEE, P-BDTPB and P-BDTPMB were calculated as 12,240, 14,500, 16,200 and 10,600 Da, respectively. The M_n values of P-BDTPP, P-BDTPEE, P-BDTPB and P-BDTPMB were determined as

9550, 10,850, 13,050 and 8350 Da. Also, PDI values of P-BDTPP, P-BDTPEE, P-BDTPB and P-BDTPMB were determined as 1.28, 1.33, 1.24 and 1.27, respectively. All of the polymers shows narrow PDI value. The narrow polydispersity value indicates that the polymerization reactions are selectively controlled (Bilici et al., 2010).

3.6. Surface morphological properties of polymers

The morphological properties of synthesized polymers were determined by using scanning electron microscope. SEM imaging was performed to observe how affect the morphological properties of the polymers containing aliphatic and aromatic groups used as bridge were affected. As seen in Fig. 10, P-BDTPP is composed of dense particles with different sizes, while P-BDTPEE is composed of sharp surfaces. In addition, layered structures were observed in P-BDTPB and P-BDTPMB where benzene and xylene dibromide compounds were used as bridges.

4. Conclusions

In conclusion, the aliphatic and aromatic bridging monomers containing phenothiazine unit were synthesized and converted into their corresponding polymers via oxidative polymerization using FeCl_3 as oxidant. While optical band gaps of the synthesized compounds were between 1.92 and 3.35 eV, electrochemical band gaps were between 1.90 and 2.96 eV. According to fluorescence measurements, fluorescence intensities of the monomers and the polymers were generally high.

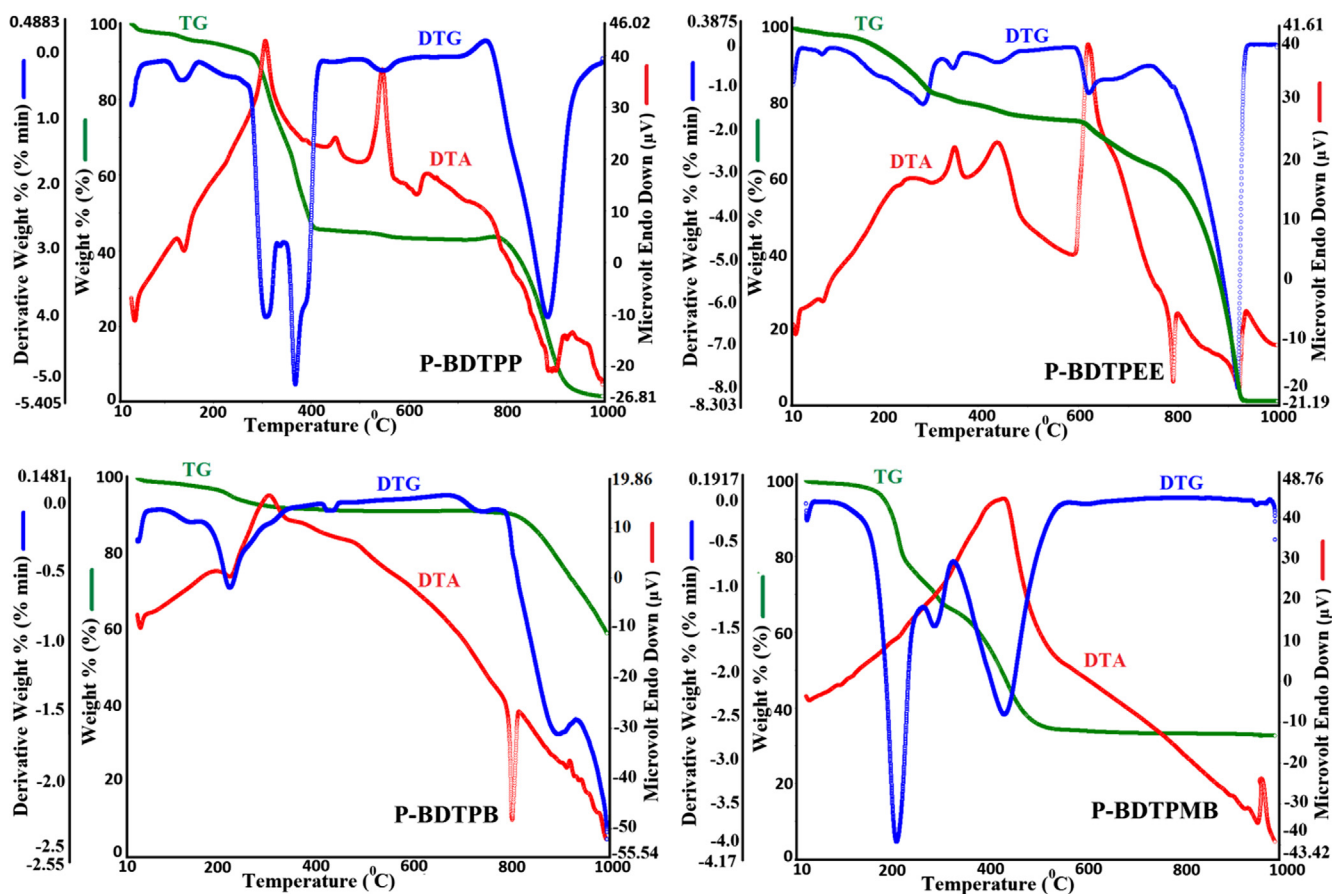


Fig. 9 TG-DTA-DTG curves of the polymers.

Table 5 Thermal analysis data of the synthesized monomers and polymers.

Compounds	^a T _{on}	^b T _{max}	^c T ₂₀	^d T ₅₀	TGA (°C)	I. Step (°C)	II. Step (°C)	III. Step (°C)	DTA (°C)
									Endo/Exo
BDTPP	192	231, 507	198	219	1.96	110–400 (90.95%)	400–1000 (7.09)	–	68,231/500, 538
P-BDTPP	282	307, 368, 882	330	422	5.88	160–455 (50.31%)	455–690 (2.32%)	690–1000 (41.47%)	140/306, 545
BDTPEE	286	261, 311, 583	298	322	–	200–395 (88.3%)	395–550 (11.7%)	–	186/337, 518
P-BDTPEE	206	290, 621, 917	440	848	3.75	150–504 (21.11%)	504–741 (12.45%)	741–1000 (62.69%)	789/353, 440, 620
BDTPMB	226	262, 583	320	555	7.06	160–405 (25.04%)	405–1000 (67.91%)	–	–/580
P-BDTPMB	189	215, 293, 435	228	428	32.64	100–268 (26.24%)	268–332 (7.97%)	332–1000 (33.15)	–/430
BDTPB	275	300, 590	326	522	1.05	100–448 (30.09%)	448–1000 (68.86)	–	173/590
P-BDTPB	196	217, 426, 891	895	–	61.25	160–390 (5.91%)	390–757 (0.82)	757–1000 (32.05%)	220, 798/299

^a The onset temperature.

^b The maxima peak temperature.

^c Temperature corresponding to 20% weight loss.

^d Temperature corresponding to 50% weight loss.

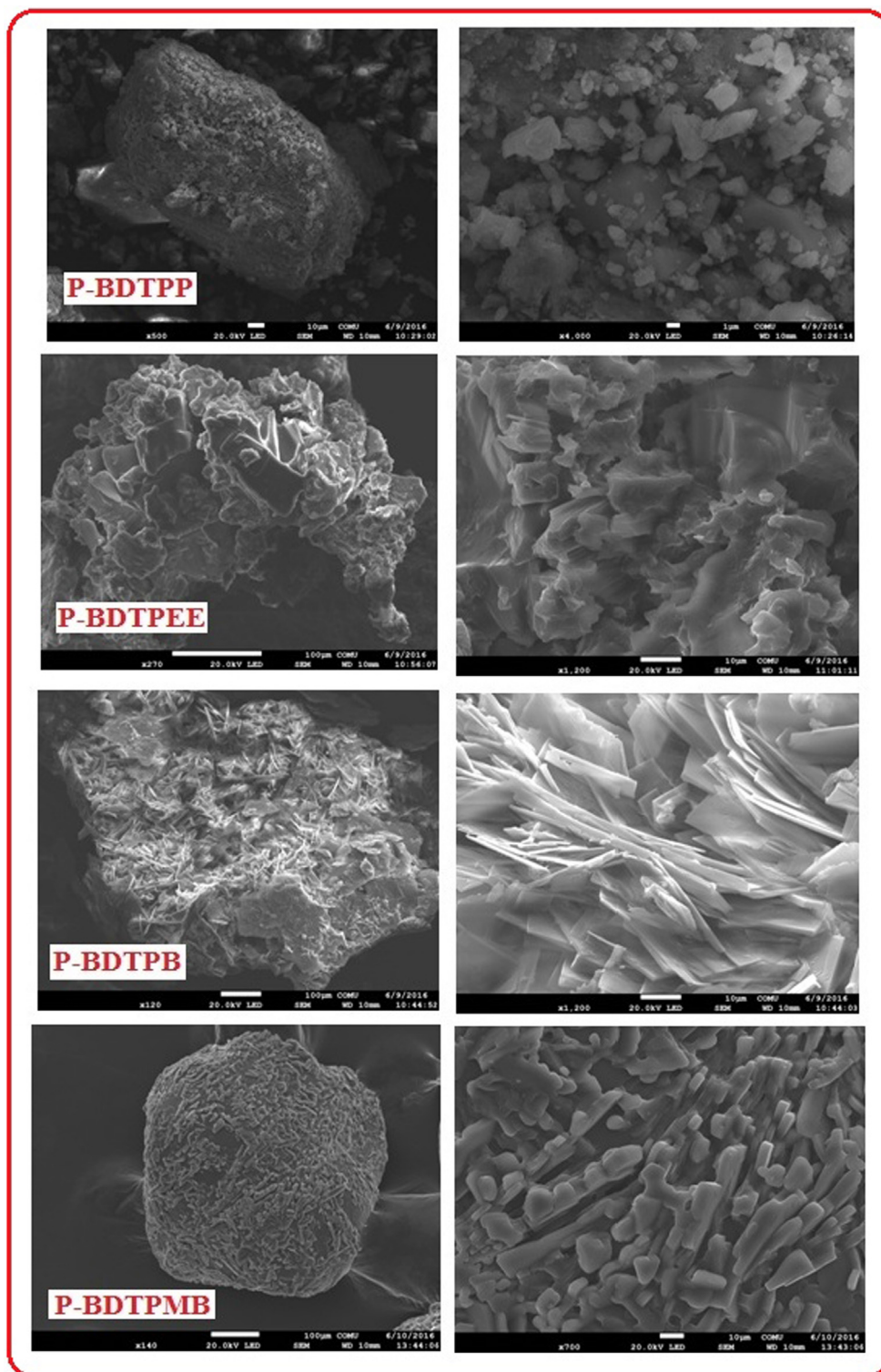


Fig. 10 SEM images of the polymers.

While P-BDTPEE had yellow color under sunlight and turned into turquoise when excited with the wavelength of 365 nm. Thermal analyses demonstrated that P-BDTPB had 38% residue amount. It can be said that, this polymer had higher thermal stability than other polymers.

Acknowledgement

The authors would like to thank Government Planning Organization for the financial support (Project No. GPO2010K120710).

References

- Aydın, A., Kaya, İ., 2013. Syntheses, characterizations and electrochromic applications of polymers derived from carbazole containing thiophene rings in side chain with electrochemical and FeCl_3 methods. *Org. Electron.* 14, 730–743.
- Bilici, A., Kaya, İ., Yıldırım, M., 2010. Biosynthesis and characterization of organosoluble conjugated poly(2-aminofluorene) with the pyrazine bridged. *Biomacromolecules* 11, 2593–2601.
- Cai, T., Zhou, Y., Wang, E., Hellström, S., Zhang, F., Xu, S., Inganäs, M.R.A., 2010. Low bandgap polymers synthesized by FeCl_3 oxidative polymerization. *Sol. Energy Mater. Sol. Cells* 94, 1275–1281.
- Cervini, R., Li, X.C., Spencer, G., Holmes, A.B., Morotti, S.C., Friend, R.H., 1997. Electrochemical and optical studies of PPV derivatives and poly(aromatic oxadiazole)s. *Synth. Met.* 84, 359–360.
- Colladet, K., Nicolas, M., Goris, L., Lutsen, L., Vanderzande, D., 2004. Low-band gap polymers for photovoltaic applications. *Thin Solid Films* 45, 7–11.
- Gao, H.-H., Qian, X., Chang, W., Wang, S.-S., Zhu, Y.-Z., Zheng, J.-Y., 2016. Oligothiophene-linked D- π -A type phenothiazine dyes for dye-sensitized solar cells. *J. Power Source* 307, 866–874.
- Hengesberg, M., Bayarmagnai, B., Jacobs, N., Bay, S., Follman, S., Wilhelm, C., Zhou, Z., Hartman, M., Müller, T.J.J., Ernst, S., Wittstock, G., Thiel, W.R., 2013. Structurally stressed PT09SBA: a close look at the properties of large pore photoluminescent, redox active mesoporous hybrid silica. *RSC Adv.* 3, 8242–8253.
- Hsieh, T.-S., Wu, J.-Y., Chang, C.-C., 2015. Multiple fluorescent behaviors of phenothiazine-based organic molecules. *Dyes Pigm.* 112, 34–41.
- Jin, Y., Liu, Y., Wu, W., Gao, H., Wang, C., Xu, S., Cao, S., 2015. Synthesis of conjugated polymers bearing pendant bipyridine ruthenium complexes. *React. Funct. Polym.* 90, 7–14.
- Jo, M.Y., Do, T.T., Ha, Y.E., Won, Y.S., Kim, J.H., 2015. Enhanced efficiency in polymer solar cells by incorporation of phenothiazine-based conjugated polymer electrolytes. *Org. Electron.* 16, 18–25.
- Kaya, İ., Temizkan, K., Aydın, A., 2013. Synthesis and characterization of aromatic and aliphatic ether bridged polymers containing carbazol moieties. *Mater. Sci. Eng. B* 178, 863–874.
- Kocaeren, A.A., 2016. Synthesis and characterization of novel polymers based on carbazole with NaOCl and FeCl_3 oxidants. *Iran. Polym. J.* 25, 15–24.
- Lin, J., Ni, X., 2015. Synthesis, structures and electrochromic behaviors of poly(triarylamine)s based on 3-substituted thiophene derivatives. *RSC Adv.* 5, 14879–14886.
- Maglione, C., Carella, A., Centore, R., Chávez, P., Lévêque, P., Fall, S., Leclerc, N., 2017. Novel low bandgap phenothiazine functionalized DPP derivatives prepared by direct heteroarylation: application in bulk heterojunction organic solar cells. *Dyes Pigm.* 141, 169–175.
- Manju, T., Manoj, N., Braun, A.M., Oliveros, E., 2012. Self sensitized photooxidation of N-methyl phenothiazine: acidity control of the competition between electron and energy transfer mechanisms. *Photochem. Photobiol. Sci.* 11, 1744–1755.
- Oleksy, A., Soloducho, J., Cabaj, J., 2011. Phenoxazine based units-synthesis, photophysics and electrochemistry. *J. Fluorescence* 21, 169–178.
- Qui, X., Lu, R., Zhou, H., Xu, X.T., Liu, X., Zhao, Y., 2007. Synthesis of linear monodisperse vinylene-linked phenothiazine oligomers. *Tetrahedron Lett.* 48, 7582–7585.
- Quiao, Z., Peng, J., Liu, Y., Weng, Q.J., He, Z., Han, S., Cao, D., 2010. Synthesis and electroluminescence properties of fluorene-co-diketopyrrolopyrrole-co-phenothiazine polymers. *Polymer* 51, 1016–1023.
- Sarhan, A.A.O., Bolm, C., 2009. Iron(III)chloride in oxidative C-C coupling reactions. *Chem. Soc. Rev.* 38, 2730–2744.
- Vengaian, K.M., Britto, C.D., Sivaraman, G., Sekar, K., Singaravadi-vel, S., 2015. Phenothiazine-based sensor for naked-eye detection and bioimaging of $\text{Hg}(\text{II})$ and F^- ions. *RSC Adv.* 5, 94903–94908.
- Yun, D.-H., Yoo, H.-S., Heo, S.-W., Song, H.-J., Moon, D.-K., Woo, J.-W., Park, Y.-S., 2013. Synthesis and photovoltaic characterization of D/A structure compound based on N-Substituted phenothiazine and benzothiadiazole. *J. Ind. Eng. Chem.* 19, 421–426.